

# Time Domain Investigation of Excited-State Vibrational Motion in Organic Molecules by Stimulated Emission Pumping<sup>†</sup>

G. Cerullo,\* L. Lüer, C. Manzoni, and S. De Silvestri

National Laboratory for Ultrafast and Ultraintense Optical Science – INFN, Dipartimento di Fisica, Politecnico di Milano, Piazza L. da Vinci 32, I-20133 Milano, Italy

O. Shoshana and S. Ruhman\*

Department of Physical Chemistry and the Farkas Center for Light Induced Processes, The Hebrew University, Jerusalem 91904, Israel

Received: December 31, 2002; In Final Form: June 23, 2003

A novel technique is demonstrated for the study of molecular vibrational dynamics in the structurally relaxed electronically excited state. The molecule is first optically excited and allowed to vibrationally relax. During the excited-state lifetime, emission is stimulated impulsively with a resonant <10-fs pulse, inducing vibrational coherence in both coupled electronic states. These are detected by an equally short probing pulse. In this first report, the methodology is applied to a substituted oligo(phenylene vinylene) in solution, and a complex vibrational response consisting of contributions from a number of active normal modes is observed. Our analysis shows that modulations observed in the experiment result mainly from vibrational coherences in the excited electronic state. The most prominent modulation is observed at 1589 cm<sup>-1</sup> and is assigned to the excited-state potential. The strong similarity of this frequency with that detected in resonant Raman scattering (1591 cm<sup>-1</sup>) supports electronic structure calculations for this class of molecules. The spectroscopic scheme demonstrated here should prove to be useful in many other systems for obtaining excited-state vibrational dynamics.

## 1. Introduction

Impulsive coherent vibrational spectroscopy (ICVS) enables one to follow vibrational motions coupled to the electronic transition of molecules and solids in real time. A femtosecond light pulse, with a duration much shorter than the rearrangement processes on the excited state, projects the ground-state multidimensional vibrational wave function onto the excited state in the form of a vibrational wave packet.<sup>1</sup> Periodical motion of localized packets formed in this way along displaced bound coordinates can in turn be followed in emission or absorption, and from them the vibrational dynamics in the excited-state can be deduced.<sup>2–4</sup>

Assuming that the excitation pulse is also significantly shorter than ground-state vibrational periods, it will simultaneously induce ground-state vibrational coherence due to resonant impulsive stimulated Raman scattering (RISRS).<sup>5–10</sup> This ubiquitous process is most easily portrayed by assuming that no ground-state nuclear motion takes place during the rapid electronic excitation. The transition can then be thought of as taking place in an array of independent two level systems, each defined at a specific point in coordinate space and characterized by a resonance frequency matching the gap between ground and excited states at that point. Accordingly the pulse leads to enhanced population transfer for molecular geometries in which the central frequency of the pulse perfectly matches the interpotential gap. The localized coherent “hole” eroded in the ground state in this fashion will later evolve similarly to the

wave packets described above and, as before, provide measures of the ground-state vibrational dynamics. Because the hole evolves in parts of coordinate space already populated, the vibronic levels participating in building up the negative interference or “hole” are naturally in the same energetic range—near the bottom of the vibrational manifold.

As a result, in a pump–probe experiment, both ground- and excited-state vibrational frequencies can be present in the transient signal because of evolution along bound vibrational coordinates in both. However, while the nascent excited state is generated far from configurational equilibrium (the most extreme case being excitation into a photodissociative state), RISRS-induced coherence provides, as described, a measure of the free induction decay of the active modes near the bottom of the vibrational ladders in the ground state. This in turn provides equivalent information to that derived from resonance Raman (RR) or spontaneous Raman spectra in a bare minimum of observation time.<sup>11,12</sup> Accordingly, RISRS has been used to follow vibrational dynamics in the ground state of both stable<sup>13,14</sup> and transient species<sup>15</sup> in very small molecules, as well as proteins.<sup>16</sup>

The need for resonant excitation limits the application of ICVS to molecules absorbing at wavelengths for which very short laser pulses are available. In particular, time domain observation of the carbon backbone stretching modes, which have 20–30 fs periods, calls for <10-fs pulses,<sup>17,18</sup> which are not readily available for the UV wavelengths at which most conjugated materials absorb. Besides, even if one could obtain the vibrational dynamics from the excited-state wave packet motion, it would teach about frequencies and relaxation rates

<sup>†</sup> Part of the special issue “A. C. Albrecht Memorial Issue”.

\* To whom correspondence should be addressed. E-mail addresses: giulio.cerullo@fisi.polimi.it; sandy@fh.huji.ac.il.

of highly excited and substantially displaced configurations of the excited state.

In this work, we report a novel approach based on a sequence of three ultrashort laser pulses, which overcomes these difficulties. A first pulse, the “pump”, resonant with the molecular absorption, brings population from the ground electronic state ( $S_0$ ) to the first excited state ( $S_1$ ); this pulse does not need to be very short and is thus readily available also in the UV region. After a certain delay, which allows the population to relax to the bottom of the excited-state potential energy surface (PES), a second ultrashort pulse, coined the “dump” pulse, resonant with the emission band of the molecule, interacts with the excited-state population, bringing it back down to the ground state. Finally a third “probe” pulse measures the changes in differential transmission induced by the dump, which reflect the RISRS “hole”, this time in the excited state.

Conceptually, this is precisely the RISRS scenario stood on its head, with a reversal in roles between the ground and excited states. Accordingly, just as RISRS is ideally capable of providing frequencies and decay times of ground-state vibrational modes near equilibrium, this inverse RISRS should be ideally suited to provide equivalent data for the excited state with the added benefit that the Stokes shift of the emission allows this spectroscopy to be conducted at longer laser wavelengths. While various ultrafast three pulse schemes have been applied to a range of dynamical problems,<sup>19–23</sup> this is the first time to our knowledge that a three-pulse sequence is specifically dedicated to obtaining excited-state vibrational dynamics.

Knowledge of the vibrational modes coupled to the electronic excited state is particularly important for  $\pi$ -conjugated polymers and oligomers, because it can help to shed light on the nature of the photoexcitations<sup>24</sup> in this technologically important class of materials.<sup>25</sup> In the excitonic picture, the photoexcitations are spatially localized and of molecular character,<sup>26</sup> so only minor changes are expected in geometry and vibrational frequencies of the excited state. In the semiconductor-band-like model, major changes in excited-state frequencies are expected as a consequence of the local redistribution of the dimerization pattern.<sup>27</sup> For strongly fluorescent molecules, it is difficult to gain this information by time-resolved excited-state RR spectroscopy because of strong background fluorescence.

The molecule studied in this work is an oligo(*p*-phenylene vinylene) with four phenyl groups (henceforth, 4PV), which is an oligomer precursor of poly(phenylene vinylene) (PPV). This class of compounds has been extensively studied as a potential constituent of organic light-emitting diodes. Vibronic coupling is fundamental to the understanding and optimization of luminescence in *n*PV (where *n* is the number of (phenylene vinylene) units) and PPV. The question of whether absorption and fluorescence are mirror images in these compounds is controversial. If dispersion<sup>28</sup> and temperature-induced torsional<sup>29</sup> effects are absent, asymmetry can only be due to an intrinsic distortion of the excited state, leading to a change in fundamental frequencies with respect to the ground state. A complete vibronic analysis of both fluorescence emission and excitation spectra was performed for the shortest *n*PV homologue, *trans*-stilbene.<sup>30</sup> It was found that for all fundamental vibrations, the frequency of C=C stretches or CCC-bend vibrations is about 30–50  $\text{cm}^{-1}$  lower in the excited state compared to the ground state. However, for vibrations higher than 1200  $\text{cm}^{-1}$ , the assignment of excited-state vibrations to fundamental frequencies was difficult because of isomerization. Because of the wealth of normal vibrations, this evaluation cannot be done with longer oligomers. However, Gierschner et al.<sup>31</sup> showed that the main

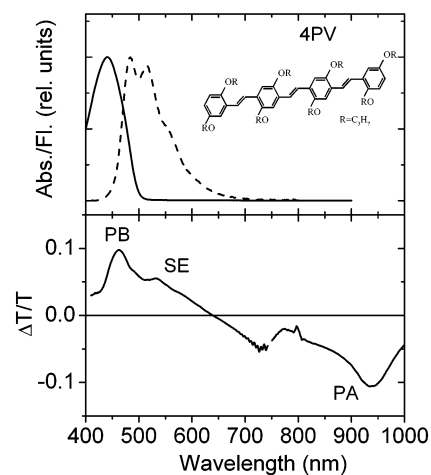


**Figure 1.** Absorption (solid line) and emission (dashed line) spectra (upper panel) of 4PV in toluene solution. The inset shows the chemical structure of the 4PV molecule. The lower panel shows the differential transmission spectrum of 4PV at 4 ps pump–probe delay.

features (i.e., all visible peaks and approximate intensities) of low-temperature fluorescence spectra of 2PV can be reproduced by considering only three prominent fundamentals. Quantum-chemical calculations for *n*PV by the same authors reveal equal frequencies but different relative intensities for the ground and excited states. The practical importance of vibronic coupling in this family of molecules, along with the difficulties in obtaining this information using standard techniques, makes them ideal candidates for a first application of the new scheme demonstrated in this report.

## 2. Experimental Section

Investigations were performed on 4PV molecules each substituted with oxypropyl side chains in the 2 and 5 positions (see inset of Figure 1 for the chemical structure). Synthesis of these molecules is described elsewhere.<sup>32</sup> Room temperature,  $\sim 2 \times 10^{-4}$  M solutions in toluene were kept in a 200  $\mu\text{m}$  path length cell, equipped with 150  $\mu\text{m}$  thick quartz windows, which limit the dispersive pulse broadening effects. The pump–probe experimental system starts with a mode-locked Ti:sapphire system with chirped pulse amplification, producing 500  $\mu\text{J}$ , 150 fs pulses at 790 nm and 1 kHz repetition rate. A fraction of the pulse energy powers a visible noncollinear optical parametric amplifier (NOPA), pumped by the second harmonic of the Ti:sapphire laser and seeded by a white light continuum.<sup>33</sup> The system generates pulses with ultrabroad bandwidth, extending from 500 to 650 nm, and energy of 1–2  $\mu\text{J}$ , compressed nearly to the transform limit producing pulses of <10-fs duration by multiple reflections onto chirped dielectric mirrors with custom-tailored dispersion.<sup>34</sup>

A fraction of the NOPA pump beam at 390 nm is split and used to excite the 4PV molecule into its first excited singlet state. After a variable delay (in the 1–60 ps range), an intense NOPA pulse, resonant with the stimulated emission of 4PV, dumps population down to the ground state; a third, weaker pulse, also derived from the NOPA, probes the subsequent system dynamics. Single wavelengths of the broadband probe pulse are selected by 10-nm bandwidth interference filters after the sample and the differential transmission ( $\Delta T/T$ ) signal is obtained combining differential detection with lock-in amplification. Our detection scheme, in which we modulate the pump pulse, allows observation only of the resonant effect of the dump

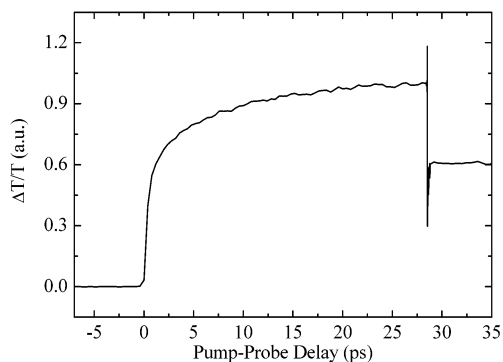


**Figure 2.** Differential transmission dynamics of 4PV in a pump-dump-probe experiment at 570 nm probe wavelength.

pulse, that is, the variation that it induces in 4PV excited-state population without the nonresonant solvent response.

### 3. Results and Discussion

The absorption and fluorescence spectra of 4PV in toluene are shown in Figure 1a as solid and dashed lines, respectively. Figure 1b shows the differential transmission ( $\Delta T/T$ ) spectrum following photoexcitation with a 200-fs pulse at 390 nm, obtained by probing with a broadband supercontinuum generated in a sapphire plate. We observe photobleaching of ground-state absorption, a broad stimulated emission (SE) band, extending from 500 to 620 nm, and a broad excited-state absorption band in the red-near-infrared spectral range. Both the SE and excited-state absorption (ESA) features are assigned to the first excited singlet state ( $S_1$ ) and decay on the time scale of a few hundred picoseconds. The  $S_1$  population can therefore be regarded as stationary on the time scale of the three-pulse experiment ( $\sim 2$  ps). The presence of two well-separated and nonoverlapping SE and ESA bands allows dumping of the  $S_1$  population to the ground state with negligible excitation of higher-lying electronic states.

Typical SE kinetics, at the wavelength of 570 nm, are displayed in Figure 2. The signal rises with the pump pulse and then shows an additional slow increase on the picosecond time scale due to conformational relaxation (to be discussed later). The dump pulse, delayed from the pump by  $\sim 28$  ps, induces a strong depletion of excited-state population, which is reflected in a sudden reduction in SE. This reduction recovers partially on a subpicosecond time scale with little subsequent change in the intensity of the SE signal. An expanded view of the SE dynamics following the dump pulse is presented in Figure 3 (upper panel), together with an exponential fit of SE recovery, giving a time constant of  $\sim 100$  fs at this wavelength. On an expanded time scale, a visible oscillatory pattern is also apparent, due to coherent vibrational motions in  $S_1$  and  $S_0$  induced by the dump pulse, as described in the Introduction.<sup>35</sup> This pattern is better displayed in Figure 3 (lower panel), after subtraction of the slowly varying background. Similar dynamics are observed throughout the SE band, as shown in Figure 4 for wavelengths ranging from the peak (510 nm) to the tail (610 nm) of the emission band.

Let us first discuss the population dynamics following the dump pulse. The pump populates a higher-lying vibronic state of  $S_1$ . A rapid intramolecular vibrational relaxation (IVR) to the bottom of the excited-state PES<sup>36</sup> is followed by an additional slower conformational relaxation, most probably due to a planarization of the molecule from a distorted ground-state configuration.<sup>37,38</sup> This energy dissipation induces a red shift in the emission spectrum, which manifests itself as an increase

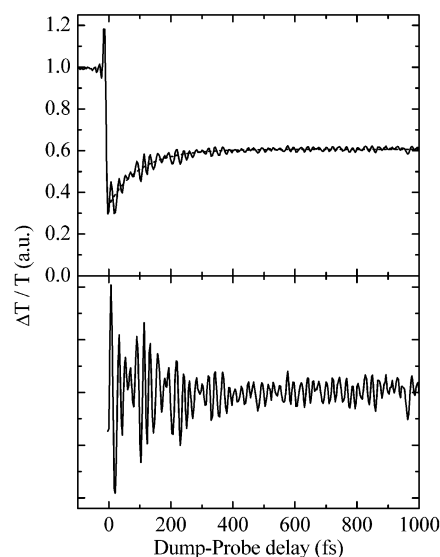


**Figure 3.** Expanded view of the  $\Delta T/T$  signal (upper panel) after the arrival of the dump pulse at 570 nm probe wavelength (solid line) and exponential fit (dashed line) and oscillatory component (lower panel) of the signal after subtraction of a slowly varying background.

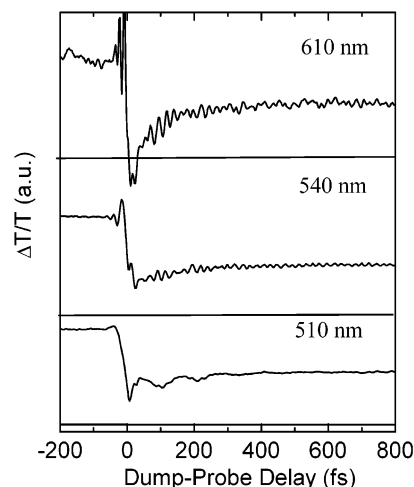


**Figure 4.**  $\Delta T/T$  dynamics following the dump pulse at different probe wavelengths spanning the emission spectrum. Solid lines indicate the zero levels for the corresponding traces.

of the red wing of stimulated emission over time. This effect is responsible for the increase of  $\Delta T$  during the first 20 ps. The dump pulse induces a decrease in excited-state population, resulting in a reduced SE signal. There is, however, a partial recovery of the SE signal over a time scale of a few hundred femtoseconds. Similar absorption replenishment has been observed in other pump-dump-probe experiments<sup>19,20</sup> and can be understood employing the Franck-Condon (FC) principle whereby the dump pulse generates a localized  $S_0$  wave packet, which absorbs precisely at the dumping frequency. This wave packet must be comprised of excited vibrational levels that are unpopulated at thermal equilibrium (there is no absorption at these wavelengths). This hot ground-state absorption results in a negative  $\Delta T/T$  signal contributing to the SE reduction, and the SE recovery therefore corresponds to a relaxation of ground-state population out of the FC window. This interpretation is supported by the observation that the recovery time slows as the detection wavelength is tuned to the blue, as evidenced in Figure 4 (it ranges from 62 fs at 610 nm to 200 fs at 510 nm). According to this interpretation, ground-state contributions to the oscillations should be over within the first  $\sim 0.5$  ps of delay.

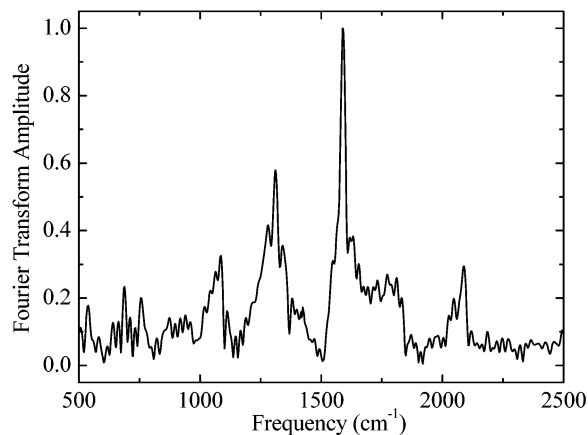


**Figure 5.** Fourier transform of the oscillatory component of the  $\Delta T/T$  signal at 570 nm.

After this time, the hot ground-state population has abandoned the FC region and the signal should exclusively reflect excited-state population.

Let us now discuss the oscillatory component of the signal, a Fourier transform of which is shown in Figure 5. We observe several peaks above the noise level in the 1000–2100  $\text{cm}^{-1}$  frequency range, centered at 1085, 1285, 1315, 1589, and 2090  $\text{cm}^{-1}$ . These spectral features are reproducible, albeit with different relative weights, at other probe wavelengths as well. The peaks are associated with vibrations of the 4PV molecule and not the solvent because the signal is referenced to the modulated pump beam, and none of the characteristic frequencies of the solvent (800, 1000  $\text{cm}^{-1}$ <sup>39</sup>) are in fact observed.

At all probe wavelengths, the strongest peak is at  $\nu_1 = 1589 \pm 1 \text{ cm}^{-1}$  and corresponds to the strongly coupled mode observed at 1591  $\text{cm}^{-1}$  in RR spectra and assigned to the C=C stretching in related compounds.<sup>40</sup> The observed spectral line presents a broad asymmetric pedestal, suggesting that it is composed of two overlapping lines with different widths. To reliably extract frequencies and damping times of the coupled modes, we analyzed the oscillatory component of the signal by a linear-prediction singular-value decomposition (LPSVD) algorithm.<sup>41</sup> While providing a perfect fit to the data, the overdetermined nature of the output requires screening of the spectral components to identify those that are physically significant and related to the vibrational dynamics. At all wavelengths, aside from  $\nu_1$ , an oscillatory component at 1534  $\text{cm}^{-1}$  is obtained in the LPSVD analysis, which always decays more rapidly than the former.

The lower frequency component is particularly interesting in view of the possibility that vibrational coherences on both electronic states are being detected. At long dump delays, we start from a relaxed excited-state configuration, and the dynamical hole burnt in the upper surface will involve vibrational levels near the bottom of the PES. On the other hand, because of the difference between ground- and excited-state equilibrium configurations, ground-state coherence will involve higher-lying levels. As discussed above, nonoscillatory ground-state contributions to the transient bleach in the emission are observed only at times shorter than  $\sim 0.5$  ps. Accordingly a ground-state component appearing at wavelengths above the absorption spectrum would be expected to decay more rapidly. On the other hand, two closely spaced LPSVD components that decay on different time scales may simply reflect a nonexponential dephasing dynamics or a slight chirp reflecting population decay of a single vibration in either of the electronic states.

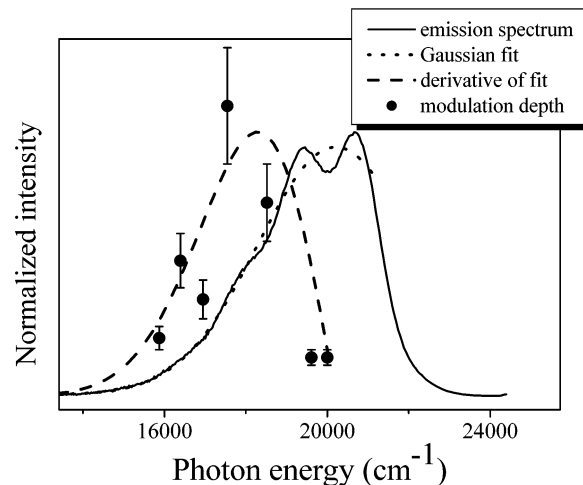


**Figure 6.** Depth of stimulated emission modulations as a function of the probing frequency, along with the emission spectrum, a Gaussian fit to that spectrum, and a first derivative of that fit.

Because no precise record of 4PV ground-state vibrational frequencies is available from a Raman spectrum, another criterion for assigning the modulations to the two involved potentials is needed. Assuming to a first approximation that the emission band of the fluorescent state is being modulated in wavelength space by the active vibrations, the resulting spectral oscillations should scale as  $d\sigma/d\nu$ ,  $\sigma$  representing the emission cross section and  $\nu$  the probing photon frequency. Similarly the phase of the modulations should change by  $\sim \pi$  as the probe is tuned from the red to the blue side of the band.<sup>7,42</sup> Modulations at the fundamental frequencies, which originate from vibronic coherences in the excited state, should become much weaker at the band maximum near 510 nm. This is not at all true of the ground-state contributions, which if anything should become more long-lived and intense as the probe is tuned to the blue where the relaxed parent absorbs.

To check this, the absolute value of the high-frequency modulation depth in the emission signal ( $\Delta T/T$ ) is plotted as a function of photon energy, along with the emission spectrum in Figure 6. To assess the adherence of this measure to the derivative of the emission intensity with  $\nu$ , the figure also includes a Gaussian fit of the emission band and its derivative, all normalized to a peak of unity. While the  $\Delta T/T$  values do not match the derivative of the emission band exactly, the trends of changes with the probing frequency match expectations from excited-state coherences. The only modulation component that does not reduce markedly in amplitude when probing near to the emission peak is that at 250  $\text{cm}^{-1}$ , suggesting that this low-frequency mode represents motions on the ground state, while all others, which fade with the blue probe, are probably assignable to the excited state.

Another method of determining where the coherences are generated is afforded by changing the time delay between the pump and dump pulses, thereby probing the vibrational dynamics at different stages of excited-state relaxation. Figure 7 shows the Fourier transforms of the oscillatory component of the signal at 570 nm probe wavelength for different pump–dump delays, ranging from 1.7 to 28 ps. Within the noise level, the spectra present very similar features. There are however observable differences between these spectra, which reflect some molecular evolution taking place during the cooling period. First, a shoulder grows in gradually around 1750  $\text{cm}^{-1}$  and, given the slow appearance of this feature, may reflect the same process that causes the slow red-shifting and, in our data, the increased



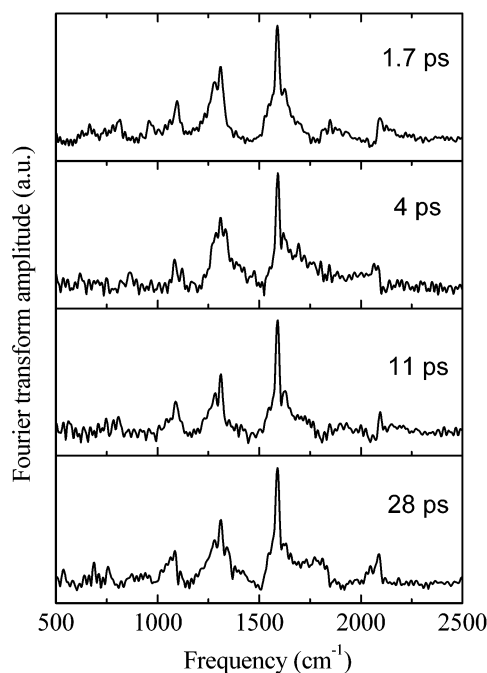


**Figure 7.** Fourier transform of the oscillatory component of the  $\Delta T/T$  signal at 570 nm probe wavelength for different pump–dump delays.

amplitude of stimulated emission over the first 60 ps. The second is an increased amplitude to the red of the  $1589\text{ cm}^{-1}$  band, which is gone already in the 4 ps data and at all later delays. This is most likely due to hot band activity and suggests that at shorter delays, more pronounced indications of excess energy deposited by the UV photon may be observable as hot bands in modes to be associated with the excited state. The somewhat disappointing absence of striking evolution in the data at the various pump–dump delays beyond 2 ps can be understood by recalling that in conjugated polymers and oligomers IVR takes place on a very short time scale ( $\ll 200$  fs), as evidenced by fluorescence upconversion experiments.<sup>36</sup>

Finally, it is worth noticing that in these experiments it is very difficult to make use of the modulation phase, because it involves a very precise determination of time zero and an error of just 1 fs implies a phase shift of almost  $20^\circ$ . Furthermore utilizing the phase would be of little use because the probe frequencies only span the red half of the emission band. A conclusive experiment is underway to put to rest the question of possible contributions to the modulations by the ground state. At the price of somewhat reduced time resolution, a similar pump–dump scheme will be executed, but instead of probing excited-state emission, probing will be conducted in the excited-state absorption. Accordingly, only the first excited state is common to the excitation and probing stages, and only coherences therein will become observable in that experiment.

## Conclusions

In this work, we have demonstrated a novel technique for the study of vibrational coherence in organic molecules, based on stimulated emission pumping using a sequence of three pulses. This technique enables extension of the time-domain study of vibrational coherence to a wide class of molecules with absorption in the UV range, where very short light pulses are not yet readily available. In addition, it provides information on vibrational dynamics of the excited state in a structurally relaxed thermal configuration. Applying this technique to a substituted oligo(phenylene vinylene) molecule in solution, we

have identified several strongly coupled modes. The most prominent one, at frequency  $\nu_1 = 1589\text{ cm}^{-1}$ , is assigned to the excited state because of its long damping time. Its frequency is very close to that of a mode observed in RR spectra, indicating that ground- and excited-state PES have very similar curvatures close to the bottom of the well.

Other frequencies observed, with shorter damping times, might reflect a chirp in the excited-state vibrational coherence but could also result from a superposition of both ground- and excited-state vibrations. Changes of the spectral modulation depth with probing frequency strongly suggest that all modulations above  $1000\text{ cm}^{-1}$  originate in excited-state coherences. In future work, we plan to extend the tuning range of the probe pulse to the red to be able to directly probe the  $S_1$  absorption and verify unequivocally the source of the observed vibrational coherences.

**Acknowledgment.** O. Shoshana and S. Ruhman acknowledge support from the *European Community – Access to Research Infrastructure action of the improving Human Potential Program*, Contract No. HPRI-CT-2001-00148 (Center For Ultrafast Science and Biomedical Optics, CUSBO). L. Lüer acknowledges a Marie Curie individual fellowship under Contract No. HPMF-CT-2001-01116. The Farkas center is funded by the Minerva Gesellschaft, GmbH, Munich, Germany.

## References and Notes

- Zewail, A. H. *J. Phys. Chem. A* **2000**, *104*, 5660.
- Taylor, A. J.; Erskine, D. J.; Tang, C. L. *Chem. Phys. Lett.* **1984**, *103*, 430.
- Fraginito, H. L.; Bigot, J. Y.; Becker, P. C.; Shank, C. V. *Chem. Phys. Lett.* **1989**, *160*, 10.
- Rubtsov, I. V.; Yoshihara, K. *J. Phys. Chem. A* **1999**, *103*, 10202.
- Chesnoy, J.; Mokhtari, A. *Phys. Rev. A* **1988**, *38*, 3566.
- Ruhman, S.; Kosloff, R. *J. Opt. Soc. Am. B* **1990**, *7*, 1748.
- Banin, U.; Ruhman, S. *J. Chem. Phys.* **1993**, *98*, 4391–4403.
- Ashkenazi, G.; Banin, U.; Bartana, A.; Kosloff, R.; Ruhman, S. *Adv. Chem. Phys.* **1997**, *100*, 229.
- Banin, U.; Bartana, A.; Ruhman, S.; Kosloff, R. *J. Chem. Phys.* **1994**, *101*, 8461.
- Gershgoren, E.; Vala, J.; Kosloff, R.; Ruhman, S. *J. Phys. Chem. A* **2001**, *105*, 5081.
- Banin, U.; Ruhman, S. *J. Chem. Phys.* **1993**, *99*, 9318.
- Johnson, A. E.; Myers, A. B. *J. Chem. Phys.* **1996**, *104*, 2497.
- Dexheimer, S. L.; Wang, Q.; Peteanu, L. A.; Pollard, W. T.; Mathies, R. A.; Shank, C. V. *Chem. Phys. Lett.* **1992**, *188*, 61.
- Wang, Z.; Wasserman, T.; Gershgoren, E.; Ruhman, S. *J. Mol. Liq.* **2000**, *86*, 229.
- Banin, U.; Kosloff, R.; Ruhman, S. *Chem. Phys.* **1994**, *183*, 289.
- Zhu, L.; Sage, J. T.; Champion, P. M. *Science* **1994**, *266*, 629.
- Cerullo, G.; Lanzani, G.; Muccini, M.; Taliani, C.; De Silvestri, S. *Phys. Rev. Lett.* **1999**, *83*, 231.
- Kobayashi, T.; Saito, T.; Ohtani, H. *Nature* **2001**, *414*, 531.
- Gai, F.; McDonald, J. C.; Anfinrud, P. A. *J. Am. Chem. Soc.* **1997**, *119*, 6201.
- Ruhman, S.; Hou, B.; Friedman, N.; Ottolenghi, M.; Sheves, M. *J. Am. Chem. Soc.* **2002**, *124*, 8854.
- Martini, I. B.; Barthel, E. R.; Schwartz, B. J. *Science* **2001**, *293*, 462.
- Frolov, S. V.; Bao, Z.; Wohlgenannt, M.; Vardeny, Z. V. *Phys. Rev. Lett.* **2000**, *85*, 2196.
- Gadermaier, C.; Cerullo, G.; Sansone, G.; Leising, G.; Scherf, U.; Lanzani, G. *Phys. Rev. Lett.* **2002**, *89*, 117402.
- Sariciftci, N. S., Ed. *Primary photoexcitations in conjugated polymers: molecular exciton versus semiconductor band model*; World Scientific Publ.: Singapore, 1997.
- Friend, R. H.; Gymer, R. W.; Holmes, A. B.; Burroughes, J. H.; Marks, R. N.; Taliani, C.; Bradley, D. D. C.; Dos Santos, D. A.; Bre' das, J. L.; Lögdlund, M.; Salaneck, W. R. *Nature* **1999**, *397*, 121.
- Kersting, R.; Lemmer, U.; Deussen, M.; Bakker, H. J.; Mahrt, R. F.; Kurz, H.; Arkhipov, V. I.; Bässler, H.; Göbel, E. O. *Phys. Rev. Lett.* **1994**, *73*, 1440.
- Heeger, A. J.; Kivelson, S.; Schrieffer, J. R.; Su, W.-P. *Rev. Mod. Phys.* **1988**, *60*, 781.

- (28) Rauscher, U.; Bäessler, H.; Bradley, D. D. C.; Hennecke, M. *Phys. Rev. B* **1990**, *42*, 9830.
- (29) Pauck, T.; Bäessler, H.; Grimme, J.; Scherf, U.; Müllen, K. *Chem. Phys.* **1996**, *210*, 219.
- (30) Syage, J. A.; Felker, P. M.; Zewail, A. H. *J. Chem. Phys.* **1984**, *81*, 4685.
- (31) Gierschner, J.; Mack, H. G.; Lüer, L.; Oelkrug, D. *J. Chem. Phys.* **2002**, *116*, 8596.
- (32) Stalmach, U.; Kolshorn, H.; Brehm, I.; Meier, H.; Lieb, J. *Ann. Chem.* **1996**, *9*, 1449.
- (33) Cerullo, G.; Nisoli, M.; Stagira, S.; De Silvestri, S. *Opt. Lett.* **1998**, *16*, 1283.
- (34) Zavelani-Rossi, M.; Cerullo, G.; De Silvestri, S.; Gallmann, L.; Matuschek, N.; Steinmeyer, G.; Keller, U.; Angelow, G.; Scheuer, V.; Tschudi, T. *Opt. Lett.* **2001**, *26*, 1155.
- (35) Note that the data after the dump pulse show significantly less noise than before. We interpret this noise reduction as follows: any random increase of probe pulse energy, due to fluctuations, will translate into an increase of the detected SE signal but at the same time will correspond to an increase in the energy of the dump pulse because probe and dump are derived from the same source. These two effects go in opposite directions and tend to cancel out.
- (36) Kersting, R.; Lemmer, U.; Mahrt, R. F.; Leo, K.; Kurz, H.; Bäessler, H.; Göbel, E. O. *Phys. Rev. Lett.* **1993**, *70*, 3820.
- (37) Lanzani, G.; Nisoli, M.; De Silvestri, S.; Tubino, R. *Chem. Phys. Lett.* **1996**, *251*, 339.
- (38) Wong, K. S.; Wang, H.; Lanzani, G. *Chem. Phys. Lett.* **1998**, *288*, 59.
- (39) Schrader, B.; Meier, W. *Atlas of organic compounds*; Verlag Chemie: Weinheim, Germany, 1974.
- (40) Tian, B.; Zerbi, G.; Schenk, R.; Müllen, K. *J. Chem. Phys.* **1991**, *95*, 3191.
- (41) Barkhuijzen, H.; De Beer, R.; Bovée, W. M. M. J.; van Ormondt, D. *J. Magn. Reson.* **1985**, *61*, 465.
- (42) Wang, Q.; Schoenlein, R. W.; Peteanu, L. A.; Mathies, R. A.; Shank, C. V. *Science* **1994**, *266*, 422.